Published in final edited form as:
J Neurosci. 2003 August 20; 23(20): 7670–7676.

Cellular Location and Circadian Rhythm of Expression of the Biological Clock Gene *Period 1* in the Mouse Retina

Paul Witkovsky[1,2], **Eleonora Veisenberger**[1], **Joseph LeSauter**[3], **Lily Yan**[7], **Madeleine Johnson**[4], **Dao-Qi Zhang**[6], **Douglas McMahon**[6], and **Rae Silver**[3,5,7]

[1]Department of Ophthalmology, New York University School of Medicine, New York, New York 10016

[2]Department of Physiology and Neuroscience, New York University School of Medicine, New York, New York 10016

[3]Department of Psychology, Barnard College, New York, New York 10027

[4]Graduate Training Program, Columbia University College of Physicians and Surgeons, New York, New York 10032

[5]Department of Anatomy and Cell Biology, Columbia University College of Physicians and Surgeons, New York, New York 10032

[6]Department of Biological Sciences, Vanderbilt University, Nashville, Tennessee 37027

[7]Department of Psychology, Columbia University, New York, New York 10027

Abstract

The cellular location and rhythmic expression of *Period 1* (*Per1*) circadian clock gene were examined in the retina of a *Per1*::GFP transgenic mouse. Mouse *Per1* (*mPer1*) RNA was localized to inner nuclear and ganglion cell layers but was absent in the outer nuclear (photoreceptor) layer. Green fluorescent protein (GFP), which was shown to colocalize with PER1 protein, was found in a few subtypes of amacrine neuron, including those containing tyrosine hydroxylase, calbindin, and calretinin, but not in cholinergic amacrine cells. A small subset of ganglion cells also contained GFP immunoreactivity (GFP-IR), but the melanopsin-containing subtype, which projects to the suprachiasmatic nuclei (SCN), lacked GFP-IR. Although the intensity of GFP-IR varied among the populations of amacrine cells at each time point that was examined, both diurnal and circadian rhythms were found for the fraction of neurons showing strong GFP-IR, with peak expression between Zeitgeber/circadian (ZT/CT) times 10 and 14. In SCNs that were examined in the same mice used for the retinal measures, the peak in GFP-IR also occurred at approximately ZT/CT 10. Our results are the first to demonstrate a circadian rhythm of a biological clock component in identified neurons of a mammalian retina.

Keywords

transgenic mouse; biological clock genes; retina; amacrine cell; melanopsin; circadian rhythm

Correspondence should be addressed to Dr. Paul Witkovsky, Department of Ophthalmology, New York University School of Medicine, 550 First Avenue, New York, NY 10016. pw20@nyu.edu.

Introduction

The importance of biological clocks in regulating daily rhythmic activities of organisms has been widely recognized. Such clocks allow the animal to anticipate daily and seasonal changes in environmental conditions and to adjust their rhythms accordingly. Circadian clocks also serve to coordinate the optimal phase of internal events of various tissues and organs. In mammals the master biological clock lies in the suprachiasmatic nuclei (SCN), but there is good evidence for one or more independent clocks in the retina (Anderson and Green, 2000; Tosini and Fukuhara, 2002).

The initial identification of a biological clock in the retina began with the demonstration, in *Xenopus*, that the activity of the rate-limiting enzyme for melatonin synthesis, aryl alkylamine *N*-acetyltransferase (AA-NAT), was governed by a circadian rhythm (Besharse and Iuvone, 1983). Subsequent work showed that AA-NAT was located in photoreceptor cells (Cahill and Besharse, 1992) and that an isolated layer of photoreceptors was capable of maintaining a circadian rhythm of melatonin production (Cahill and Besharse, 1993). More recent studies on *Xenopus* retina have identified multiple clock components, all of which are located exclusively in the photoreceptors (for review, see Anderson and Green, 2000).

The mammalian retina also exhibits circadian rhythms of melatonin production (Tosini and Menaker, 1996); however, the cellular location (or possibly multiple locations) of the circadian clock(s) has not been identified yet. In contrast to the *Xenopus* retina, the distribution of message for clock genes such as *clock*, *Bmal1*, and *Period 1* (*Per1*) is widespread among the retinal layers (Gekakis et al., 1998; Namihira et al., 2001), and the mRNA for the cryptochrome genes *cry1* and *cry2*, which are essential components of the molecular circadian clock mechanism (Van der Horst et al., 1999), are located in the inner retina rather than in the photoreceptors (Miyamoto and Sancar, 1998). These differences suggest that mammalian and *Xenopus* retinas may use different organizational principles in relation to their biological clocks.

An important first step in understanding the mammalian retinal biological clock is to identify precisely which mammalian retinal cell types possess circadian clock function. We have studied this question by using a transgenic mouse in which a short half-life green fluorescent protein (GFP) reporter is driven by the promoter of the *Per1* circadian clock gene (Kuhlman et al., 2000). We find *Per1*-driven GFP and PER1 protein immunostaining in the amacrine and ganglion cell layers, but not in the photoreceptor layer. Using double-label immunocytochemistry, we find that subsets of amacrine cell types, among them the dopaminergic amacrine cell, contain *Per1*-driven GFP. Additionally, we demonstrate that these cells exhibit diurnal and circadian rhythms of GFP expression. Our study is thus the first to show a circadian rhythm of a biological clock gene in identified subtypes of mammalian retinal neurons.

This work has been published in abstract form (LeSauter et al., 2002).

Materials and Methods

Animals

Hemizygous *Per1*::GFP transgenic mice (characterized by Kuhlman et al., 2000) were housed individually in translucent propylene cages in a 12 hr light/dark (LD) cycle for at least 3 weeks before use. At 4 hr intervals [Zeitgeber (ZT) or circadian (CT) 2, 6, 10, 14, 18, and 22] the mice were anesthetized deeply with 200 mg/kg pentobarbital and perfused intracardially with 50 ml of 0.9% saline, followed by 100 ml of 4% paraformaldehyde in 0.1 M phosphate buffer (PB), pH 7.3. Mice killed during the dark period were anesthetized in the

dark and had their heads covered with a light-proof hood throughout perfusion. For the CT experiments the animals were killed on day 3 of complete darkness (DD). The eyes were removed and hemisected to remove cornea and lens; the eyecups were fixed for an additional 1 hr and then washed three times for 20 min each in PB. Thereafter, either the retinas were removed for processing as whole mounts, or the eyecups were protected in 30% sucrose overnight and cryosectioned at 14 μm.

Immunocytochemistry

Sections or whole mounts were incubated for 1 hr in a blocking solution (0.1% Na-azide, 0.1% Triton X-100, 1% bovine serum albumin). Then the sections were incubated overnight in the primary antibody, whereas whole mounts were incubated for 36–48 hr at room temperature on a slowly (2–5 cycles/min) rotating table. The antibodies used were rabbit polyclonal anti-GFP (1:20,000; Molecular Probes, Eugene, OR); mouse monoclonal anti-tyrosine hydroxylase (TH; 1:500; Chemicon, Temecula, CA); rabbit polyclonal anti-PER1 (1:5000; a generous gift of Dr. S. M. Reppert, Harvard Medical School, Boston, MA); mouse monoclonal anti-calbindin (1:1000; Sigma, St. Louis, MO); goat polyclonal anti-choline acetyltransferase (1:200; Chemicon); rabbit anti-melanopsin (1:2000; a generous gift of Dr. M. D. Rollag, Uniformed Services University); and goat polyclonal calretinin (1:2000; Chemicon). Secondary antibodies included appropriately conjugated Cy3 (1:200; Jackson Laboratories, West Grove, PA) and Alexa 488 (1:400, Molecular Probes). After exposure to the primary antibody the tissue was washed in PBS six times for 10 min each and incubated for 2 hr in the fluorescent secondary. After a final series of washes the sections or whole mounts were covered in Vectashield (Vector Laboratories, Burlingame, CA) and viewed in a fluorescent microscope equipped with a digital camera. Images were processed via Adobe Photoshop/Illustrator.

Colocalization of GFP-immunoreactive (GFP-IR) and PER1-IR (both antibodies made in rabbit) was performed by the tyramide method (Shindler and Roth, 1996), using a commercially available kit (NEL 701A, PerkinElmer Life Sciences, Boston, MA). Retinas first were immunoreacted for PER-IR at 1:50,000 (one-tenth the concentration used without amplification) and then reacted successively with biotinylated goat-anti rabbit IgG, streptavidin-HRP, and Cy3-labeled tyramide. Thereafter, the second primary antibody (anti-GFP) was applied at 1:20,000 and processed as described above for single antibodies. Control experiments in which the secondary of the second antibody was shown not to react with anti-GFP or anti-PER1 antisera at one-tenth their normal concentration were reported in an earlier study (LeSauter et al., 2003). The identical procedure was used for colocalization of melanopsin-IR and GFP-IR. Melanopsin was applied at 1:20,000; the rest of the procedure was identical to that just described.

The SCN was examined from brains postfixed for 18–24 hr at 4°C and then cryoprotected in 20% sucrose in 0.1 M PB overnight. Coronal sections (40 μm) were processed free-floating. Alternate sections were incubated with rabbit polyclonal GFP (1:40,000) and processed as above, using diaminobenzidine (DAB) as the chromogen.

In situ hybridization

The *mPer1* cDNA fragment-containing vectors (a gift of Dr. Okamura, Kobe University, Japan) were linearized with restriction enzymes and then used as templates for sense or antisense cRNA probes. Digoxigenin-labeled probes were made by using digoxigenin-UTP (Boehringer Mannheim, Mannheim, Germany) with a standard protocol for cRNA synthesis (Yan et al., 1999). Mice (n = 5 in 3 *in situ* runs) were anesthetized deeply with pentobarbital (200 mg/kg) and perfused intracardially with 10 ml of autoclaved ice-cold saline, followed by 20 ml of 4% paraformaldehyde in 0.1 M PB, pH 7.4. The eyes were removed and

postfixed for 16 hr at 4°C; the retina was isolated and cryoprotected in 0.1 M PB with 20% sucrose for 48 hr. Frozen sections of retina (25 μm) were made on a Reichert–Jung cryostat (Leica Microsystems, Heidelberg, Germany).

The *in situ* hybridization histochemistry was performed as described previously (Yan and Silver, 2002). Briefly, tissue sections were processed with proteinase-K (1 mg/ml) for 10 min at 37°C, followed by 0.25% acetic anhydride for 10 min at room temperature. The sections then were incubated in hybridization buffer [60% formide, 10% dextran sulfate, 10 mM Tris-HCl, pH 8.0, 1 mM EDTA, 0.6 M NaCl, 500 mg/ml 0.2% laurylsarcosine, 200 mg/ml tRNA, 1× Denhardt's, 0.25% SDS, and 10 mM dithiothreitol (DTT)] containing the digoxigenin-labeled *mPer1* sense and antisense probes for 16 hr at 60°C. After a high-stringency posthybridization wash the sections were treated with RNase A and then were processed further for immunodetection with a nucleic acid detection kit (Boehringer Mannheim). Sections were incubated at 4°C in alkaline phosphatase-conjugated digoxigenin antibodies diluted 1:5000 in buffer A (100 mM Tris-HCl, pH 7.5, and 150 mM NaCl) for 3 d. Thereafter, the sections were washed two times for 10 min each in buffer B [containing (in mM) 100 Tris-HCl, pH 9.5, 100 NaCl, 50 $MgCl_2$] for 5 min. They then were incubated in a nitroblue tetrazolium salt solution (0.34 mg/ml) containing 5-bromo-4-chloro-3-indolyl phosphate toluidinium salt (0.18 mg/ml; Boehringer Mannheim) for 16 hr. The colorimetric reaction was stopped by immersing the sections in TE buffer, which contained the following (in mM): 10 Tris-HCl and 1 EDTA, pH 8.0.

Ganglion cell labeling

Ganglion cells were labeled by a stereotaxic injection of 0.3 μl of DiI (10 μg/ml; Molecular Probes) into either the superior colliculus or the lateral geniculate nucleus of anesthetized mice and allowing 3–5 d for transport to the retina. DiI was detected in unfixed retinal whole mounts by using a rhodamine filter set during conventional fluorescence imaging or by 543 nm laser excitation and 560 nm long-pass emission filtering in confocal microscopy on a LSM5 PASCAL confocal system mounted on an Axioskop FS2 microscope (Zeiss, Thornwood, NY). No labeling of cells was detected in the inner nuclear layer, indicating a lack of trans-synaptic transport of DiI. GFP was visualized by using either a narrow-band EGFP filter set (Chroma 41020) for conventional fluorescence or 488 nm laser excitation and 505–530 bandpass emission filtering. For Lucifer yellow (LY) injections, GFP^+ neurons in the ganglion cell layer of retinal whole mounts were visualized with a Zeiss Axioskop FS2 microscope equipped with IR-DIC and fluorescence optics. Sharp electrodes were filled with 1% LY dissolved in 140 mM LiCl with a resistance of ~50 MΩ in Ames medium at 32°C. After penetration the cells were filled by inducing amplifier oscillation via overcompensation. LY was visualized in confocal microscopy, using 488 nm laser excitation and a 505 nm long-pass emission filter.

Analysis

The NIH Image version 1.61 program was used to measure the intensity of staining in the SCN and in retinal flat mounts. Brain or retinal images were captured with a CCD video camera (Sony XC77) attached to a light microscope (Olympus BH-2). Five sections from rostral to caudal regions of the SCN and one image from each retinal quadrant were analyzed for each animal. Measurements of relative optical density (ROD) of the GFP signals in retina or SCN were obtained. Nonspecific background staining outside the GFP-labeled region was measured and subtracted from the GFP signal. The net relative ROD value for each brain section or retinal image was expressed as the percentage of maximum value in that animal. One-way ANOVA was used to test for time of day effects. For every set of ROD measurements the observer was ignorant of the ZT or CT time at which the tissue was obtained.

In other experiments the retinas were processed for the combination of GFP-IR/TH-IR or PER1-IR/TH-IR and viewed in whole mounts. For each retina that was examined, 100 dopaminergic neurons were selected at random, taking some from each retinal quadrant. GFP-IR in the dopaminergic neurons was scored either as absent/dim or medium/bright by an observer ignorant of the times at which the animals were killed. Each ZT time point was assessed in two retinas from two different animals.

Results

Total GFP-IR in retina and SCN

In an initial study of this transgenic mouse, Kuhlman et al. (2000) reported the presence of *Per1*-driven GFP in the retina. Here we characterize the distribution of GFP-IR in detail. Figure 1 illustrates the distribution of GFP-IR in the SCNs (top row) and the retinas (second row) of the same mice, killed at either CT 10 or CT 22. The retinas are viewed in flat mount, with the focal plane at the border of the inner nuclear/inner plexiform layers where amacrine cell bodies are concentrated. Many cells, having diverse sizes and shapes, showed GFP-IR, and the intensity of immunostaining varied greatly among the population of stained neurons. However, for both SCN and retina the overall level of GFP-IR is clearly much greater at ZT 10 than at ZT 22.

GFP-IR was expressed primarily in neuronal perikarya, but in some neurons the immunoreaction extended to the primary dendrites, which were made visible for 10–50 μm (data not shown). Figure 1, third row, illustrates comparable data for retinas harvested at ZT 10 and ZT 22. As for the CT data set, immunostaining is greater at ZT 10 than at ZT 22. Figure 1, bottom panel, illustrates GFP-IR in a vertical section of the retina. The labeled perikarya are found at the border of the inner nuclear/inner plexiform layers and also in the ganglion cell layer, but not in the outer nuclear layer, which consists of photoreceptor cell bodies.

The numbers of cells in the amacrine cell layer showing any GFP-IR varied from 1600 to 4000/mm^2 in retinas taken from mice killed at different ZT times. On the basis of an estimate (Jeon et al., 1998) that mouse retinas contain 60,000 cells/mm^2 in the amacrine cell layer, the GFP-IR neurons constitute 2.6–6.7% of the total. The density of GFP-IR cells in the ganglion cell layer was much lower, amounting to 43–355 cells/mm^2. According to Jeon et al. (1998), there are ~10,000 cells/mm^2 in the ganglion cell layer, so the GFP-IR neurons make up ~0.4–3.6% of the total. The question of whether GFP-IR neurons in the ganglion cell layer are true ganglion cells or displaced amacrine cells is considered below.

In another set of experiments the retinas (n = 4) were marked by a needle puncture in the mid-dorsal region to permit identification of retinal quadrants so that the density of GFP-IR cells in different retinal quadrants could be assessed. No statistically significant differences were found, i.e., GFP-IR cells are distributed more or less homogeneously across the retina, with the exception that the extreme retinal margins have a slightly lower density of GFP-IR neurons.

Distribution of *Per1* mRNA and PER1 protein in the retina

Because we observed no *Per1*::GFP reporter in the outer nuclear (photoreceptor) layer, whereas a previous study (Gekakis et al., 1998) found *Per1* mRNA there, we examined the distribution of *Per1* mRNA by *in situ* hybridization and PER1 protein gene product by immunocytochemistry in retinas from our mouse line. These experiments were conducted on retinas harvested at ZT 9, a time when Northern analysis showed that *Per1* mRNA peaks in the retina (Shearman et al., 1997). *Per1* mRNA was detected throughout the inner nuclear

layer and in specific neurons of the ganglion cell layer but was not detected in the photoreceptors (Fig. 2).

The distribution of PER1 protein was measured by immunocytochemistry and found to be confined to the border of inner nuclear and inner plexiform layers (i.e., among the amacrine cell bodies) and within the ganglion cell layer. Thus all three methods of detection yielded a consistent overall pattern of *Per1* expression in the inner nuclear and ganglion cell layers, with no detectable expression in the photoreceptors.

Two methods were used to assess whether GFP-IR and PER1-IR were found in the same cells. First we used the tyramide method of amplification and observed that GFP-IR and PER1-IR colocalized (Fig. 3). These data obtained on transverse sections provided only a small sample of the total population of GFP-IR neurons, so we could not conclude with certainty that the two antibodies invariably colocalized throughout the retina. As an additional test, however, we found that both GFP and PER1 antibodies reacted with the dopaminergic amacrine cells in the retina. This subpopulation of amacrine cells is identified uniquely by their immunoreactivity to an antibody against tyrosine hydroxylase (for review, see Witkovsky and Schuette, 1991).

GFP-IR in diverse subtypes of amacrine cell

Besides the dopaminergic amacrine cells, a number of other amacrine cell subtypes can be identified by immunocytochemical markers. For example, unique populations of so-called “star-burst” cholinergic cells are identified by an antibody against choline acetyltransferase (Famiglietti and Tumosa, 1987). On the other hand, antibodies against calcium-binding proteins, such as calbindin, immunostain a variety of amacrine cells (Haverkamp and Wässle, 2000). Figure 4 presents a composite of the antibodies used and the results obtained. We observed that dopaminergic (Fig. 4*a*), calretinin-IR neurons (Fig. 4*b*) and calbindin-IR neurons (Fig. 4*c*) in amacrine and ganglion cell layers colocalized GFP-IR. In contrast, cholinergic neurons invariably lacked GFP-IR (data not shown).We did not perform a systematic study of GFP-IR in each amacrine neuronal subpopulation at all of the ZT times; all of the measurements were made on retinas killed between ZT 6 and ZT 10, when GFP-IR is generally high (see below). These data indicate that GFP-IR is found in at least a few subtypes of amacrine cell. It is important to note that, within an amacrine cell class expressing GFP-IR, typically less than one-half of the cells in the group were GFP immunoreactive. Other subtypes, e.g., the cholinergic amacrine cells, invariably lacked GFP-IR.

GFP-IR in the ganglion cell layer

We next examined whether the population of GFP-IR neurons with perikarya in the ganglion cell layer consisted of true ganglion cells, of amacrine cells displaced to the ganglion cell layer, or of a mixture of these two groups. In that regard, Jeon et al. (1998) reported that 59 ± 4% of neurons in the ganglion cell layer of the mouse retina are displaced amacrine cells. We tested whether ganglion cells showed *Per1* expression by examining retinas ($n = 7$) in which ganglion cells were labeled retrogradely with DiI injected into the superior colliculus or lateral geniculate nucleus. A small proportion (0.5%) of DiI-labeled ganglion cells expressed *Per1*-driven GFP (Fig. 5*a*; $n = 2160$ DiI-filled cells). As an additional confirmation of the identity of the cell, some GFP neurons in the ganglion cell layer were injected with LY and then examined by confocal microscopy to verify the presence of an axon. Figure 5*b* shows a GFP^+ LY-injected cell that bears an axon. Using these approaches, we found that 11% of GFP^+ cells in the ganglion cell layer are ganglion cells. Thus although our findings clearly demonstrate the presence of *Per1*-driven GFP in a subset of ganglion

cells, the preponderance of *Per1* transcriptional activity in the ganglion cell layer is located in displaced amacrine cells.

One ganglion cell subpopulation of particular interest is the melanopsin/PACAP-containing ganglion cells that constitute the retinal projection to the SCN (Hannibal et al., 2002; Hattar et al., 2002). We tested for colocalization of GFP-IR with melanopsin-IR by using tyramide amplification. Figure 5*c* illustrates a vertical retinal section containing two ganglion cells showing melanopsin-IR (red) but lacking GFP-IR (green), which is present in neighboring neurons. Figure 5*d* is a tangential section through the border of the inner nuclear and inner plexiform layers. A displaced melanopsin-IR ganglion cell is seen to lack GFP-IR, whereas many neighboring amacrine cells show GFP-IR. A survey of all of the melanopsin-labeled neurons revealed that none showed GFP-IR.

Rhythmic expression of GFP-IR in the retina

The foregoing results identified amacrine and ganglion cells as sites of expression of the biological clock gene *Per1* in the mouse retina. To implicate these products in circadian clock function, we tested for rhythmic expression of *Per1* in neuronal populations. Mice were maintained on an LD 12 hr light/dark cycle, and the animals were harvested at 4 hr intervals, beginning at ZT 2. When the total number of neurons in the amacrine cell layer of the retina showing GFP-IR was plotted against ZT time, without regard to the intensity of the immunoreaction, no rhythm was observed (data not shown). In contrast, when the intensity of the immunoreaction as measured by theRODof GFP-IR was plotted against ZT time for the same amacrine cell population (see Materials and Methods), it did exhibit a diurnal rhythm of expression (Fig. 6, left). GFP-IR was relatively low at ZT 2, rose to a peak near ZT 10, and fell off at later times. These data indicate that, although the total number of cells exhibiting baseline *Per1* transcriptional activity detectable by the GFP reporter does not vary with time of day, the amount of *Per1*-driven gene product is rhythmic in neurons with supra-baseline levels of *Per1* activity. We further determined that, in the SCNs of the same animals used to generate the retinal data of Fig. 6, GFP-IR in the SCN peaked near ZT 10 (data not shown). The same measures were repeated on animals kept in DD for 3 d as a way of testing whether the rhythms in *Per1* gene expression were driven by the daily light/dark cycle or were the result of an endogenous circadian clock. As shown in Figure 6, right, the rhythm was maintained in DD for the total population of GFP-IR-expressing cells. We also found the same circadian rhythm of GFP-IR in the SCN (data not shown).

We used the dopaminergic neurons for further investigation because they constitute a unique set of easily identifiable amacrine cells, one that has been strongly implicated in rhythmic processes in the retina (for review, see Besharse et al., 1988). The ROD method cannot be applied to a subpopulation of cells. Instead, an observer blind to the ZT or CT time of the preparation scored the GFP-IR in dopaminergic cells as absent/dim or medium/bright. Figure 7 (light bars in left panel) shows that in this subpopulation the medium/bright GFP-IR neurons have approximately the same diurnal rhythm as does the entire population of GFP-immunoreactive amacrine neurons (compare with Fig. 6). A similar rhythm of GFP-IR was seen after 3 d in DD (dark bars in Fig. 7, left). The same measures were performed for PER1-IR at ZT times, using the companion retina from the mice used to measure GFP-IR; the results (Fig. 7, right) indicate that PER1-IR follows the same general pattern of temporal expression as does GFP-IR, although a much smaller fraction of the total had bright PER1-IR, and at ZT 18 and ZT 22, no bright PER1-IR neurons were observed. A statistical analysis of these data indicates that significant differences exist between peak times (CT/ZT 10, 14) and CT/ZT 2 or CT/ZT 22 for all data sets.

Discussion

These are the main conclusions of this study. (1) The circadian clock gene, *Per1*, as expressed by *Per1* promoter-driven GFP and by PER1 protein, was found in a few subtypes of amacrine cell and a small group of ganglion cells but was absent in photoreceptors. (2) There is a circadian rhythm of *Per*1-driven GFP and of PER1, the expressions of which are relatively low at the outset of the day (CT 0), rise to a peak between CT 10 and 14, and then wane, reaching a low point between CT 18 and 22. The collective GFP-immunoreactive populations of amacrine cells, the subpopulation of dopaminergic amacrine neurons, and the GFP-expressing neurons in the SCN all showed the same rhythm of GFP-IR. A previous study (Shearman et al., 1997) examining *mPer1* mRNA in the mouse eye noted a peak near CT 9. This time point is consistent with our data, considering that message would be expected to peak earlier than its protein product.

Biological clock genes in the retina

There is solid evidence that vertebrate retinas contain one or more biological clocks (for review, see Anderson and Green, 2000; Tosini and Fukuhara, 2002). These intrinsic pacemakers control the circadian rhythmicity of certain retinal functions, such as *N*-acetyltransferase expression and melatonin synthesis (Besharse and Iuvone, 1983), synthesis of the cone pigment, iodopsin (Pierce et al., 1993), and outer segment disk shedding by rods (Terman et al., 1993). These data notwithstanding, there is still only meager evidence concerning the anatomical localization of molecular clock components and clock function within the vertebrate retina. In the *Xenopus* retina it was concluded that photoreceptors contained a circadian clock, because photoreceptors from that retina maintain a circadian rhythm of melatonin synthesis even when studied in isolation (Cahill and Besharse, 1993). More recently, Zhu et al. (2000) found that the *Xenopus* homolog of the *clock* gene is expressed strongly in both rod and cone photoreceptors and is expressed weakly in the neural layers of the *Xenopus* retina.

In contrast, our results indicate that, in the mouse retina, expression of the clock gene *Per1* is detectable in the neural layers, but not in the photoreceptors. Previous work suggests that a variety of circadian clock genes may be distributed differentially in mammalian retinas. For example, in the mouse retina Gekakis et al. (1998) showed that *clock*, *Bmal1*, and *mPer1* transcripts were expressed strongly in photoreceptor and inner nuclear layers, with additional weaker expression in the ganglion cell layer. *Per1* and *Per2* RNA also are distributed widely among all of the nuclear layers in the rat retina (Zhuang et al., 2000; Namihira et al., 2001). Our data differ from those of Gekakis et al. (1998) in finding no *mPer1* in the outer nuclear (photoreceptor) layer, perhaps as a consequence of methodological differences. We note, however, that our data are internally consistent in that photoreceptors lacked not only *mPer1* message but also GFP-IR and PER1-IR. Our data lead us to conclude that the neural inner retina of the mouse is a likely location for a biological clock. In support of this idea we note that other critical clock genes, the cryptochromes, have been localized exclusively to the inner retina of the mouse (Miyamoto and Sancar, 1998).

Our finding that there is a circadian rhythm of *Per1*-driven GFP expression and PER1 protein in calbindin-positive, calretinin-positive, and dopaminergic amacrine cells demonstrates, for the first time in a mammalian retina, clock genes in a few identified retinal cell types, indicating that these cells are possible loci for inner retinal circadian clocks. In that regard it may be significant that the tyrosine hydroxylase-positive neurons have a circadian rhythm of dopamine production (Doyle et al., 2002a), a rhythm that persists in dystrophic rats showing severe photoreceptor degeneration. Melatonin is known to play an important role in the release of dopamine, and Niki et al. (1998) provided evidence that in

the rat retina AA-NAT, the rate-limiting enzyme for melatonin synthesis, was found in the photoreceptor layer. Doyle et al. (2002a) have used these data to argue that photoreceptors influence the amount of dopamine, but not the rhythm of its synthesis. On the other hand, retinal dopamine rhythms are blunted in a mouse strain lacking melatonin, suggesting a possible interdependence of dopamine and melatonin rhythms (Doyle et al., 2002b). Further experimentation is necessary to define fully the relative roles of various cell populations contributing to rhythmic behavior in mammalian retinas.

Possible function of biological clock proteins in retinal amacrine cells

Biological clocks in the retina presumably have two main coordinating functions. The first is intrinsic to the retina and is evidenced by the findings that many molecules of importance to retinal function and many retinal activities have a circadian rhythm of expression (summarized in Tosini and Fukuhara, 2002). In many of the studies, including our own, the eyes were not separated from the animal, permitting a possible centrifugal influence of the SCN on the retina. However, with regard to melatonin production, cultured eyes clearly retain their circadian rhythm (Cahill and Besharse, 1993; Tosini and Menaker, 1996). Moreover, Terman et al. (1993) found that the rhythm of rod disk shedding was not affected by lesions of the SCN.

A second potential coordinating role for retinal clocks is in relation to the SCN, with which the retina interacts by synchronizing it to the daily rhythm of light and darkness (Lee et al., 2003). Whether this synchronization requires the participation of a retinal clock remains to be worked out. It was demonstrated recently that a set of ganglion cells belonging to the retinohypothalamic tract expresses melanopsin (Hannibal et al., 2002; Hattar et al., 2002) and that these neurons can respond to light directly (Berson et al., 2002). We found that the melanopsin-containing ganglion cells did not express GFP-IR. On the other hand, these specialized ganglion cells send dendrites into the inner plexiform layer (Berson et al., 2002; Provencio et al., 2002), where they intermingle with amacrine cell processes and receive synaptic inputs. It is thus possible that amacrine cells, the activity of which is modulated by clock genes, influence the responsiveness of melanopsin-containing ganglion cells.

Acknowledgments

This work was supported by New York University School of Medicine Grant EY 03570 (to P.W.), Vanderbilt University Grants MH06334 and EY 09256 (to D.M.), and Barnard College Grant NS 37919 (to R.S.); Research to Prevent Blindness, Incorporated; and The Hoffritz Charitable Trust. We thank Drs. S. M. Reppert and M. D. Rollag for gifts of antibodies and Drs. F. Dunn and D. Berson for helpful advice.

References

Anderson FE, Green CB. Symphony of rhythms in the *Xenopus laevis* retina. Microsc Res Tech. 2000; 50:360–372. [PubMed: 10941172]

Berson DM, Dunn FA, Takao M. Phototransduction by retinal ganglion cells that set the circadian clock. Science. 2002; 295:1070–1073. [PubMed: 11834835]

Besharse JC, Iuvone PM. Circadian clock in *Xenopus* eye controlling retinal serotonin *N*-acetyltransferase. Nature. 1983; 305:133–135. [PubMed: 6888555]

Besharse JC, Iuvone PM, Pierce ME. Regulation of rhythmic photoreceptor metabolism: a role for post-receptoral neurons. Prog Retin Res. 1988; 7:21–61.

Cahill GM, Besharse JC. Light-sensitive melatonin synthesis by *Xenopus* photoreceptors after destruction of the inner retina. Vis Neurosci. 1992; 8:487–490. [PubMed: 1586650]

Cahill GM, Besharse JC. Circadian clock function localized in *Xenopus* retinal photoreceptors. Neuron. 1993; 10:573–577. [PubMed: 8476609]

Doyle SE, McIvor WE, Menaker M. Circadian rhythmicity in dopamine content of mammalian retina: role of the photoreceptors. J Neurochem. 2002a; 83:211–219. [PubMed: 12358745]

Doyle SE, Grace MS, McIvor W, Menaker M. Circadian rhythms of dopamine in mouse retina: the role of melatonin. Vis Neurosci. 2002b; 19:593–601. [PubMed: 12507326]

Famiglietti EV, Tumosa N. Immunocytochemical staining of cholinergic amacrine cells in rabbit retina. Brain Res. 1987; 413:398–403. [PubMed: 3300857]

Gekakis N, Staknis D, Nguyen HB, Davis FC, Wilsbacher LD, King DP, Takahashi JS, Weitz CJ. Role of the CLOCK protein in the mammalian circadian mechanism. Science. 1998; 280:1564–1569. [PubMed: 9616112]

Hannibal J, Hindersson P, Knudsen SM, Georg B, Fahrenkrug J. The photopigment melanopsin is exclusively present in pituitary adenylate cyclase-activating polypeptide-containing retinal ganglion cells of the retinohypothalamic tract. J Neurosci. 2002; 22:1–7. [PubMed: 11756482]

Hattar S, Liao H-W, Takao M, Berson DM, Yau K-W. Melanopsin-containing retinal ganglion cells: architecture, projections, and intrinsic photosensitivity. Science. 2002; 295:1065–1070. [PubMed: 11834834]

Haverkamp S, Wässle H. Immunocytochemical analysis of the mouse retina. J Comp Neurol. 2000; 424:1–23. [PubMed: 10888735]

Jeon C-J, Strettoi E, Masland RH. The major cell populations of the mouse retina. J Neurosci. 1998; 18:8936–8946. [PubMed: 9786999]

Kuhlman SJ, Quintero JE, McMahon DG. GFP fluorescence reports *Period1* circadian gene regulation in the mammalian biological clock. NeuroReport. 2000; 11:1–4. [PubMed: 10683819]

Lee HS, Nelms JL, Nguyen M, Silver R, Lehman MN. The eye is necessary for a circadian rhythm in the suprachiasmatic nucleus. Nat Neurosci. 2003; 6:111–112. [PubMed: 12536213]

LeSauter J, Veisenberger E, Johnson M, McMahon D, Silver R, Witkovsky P. Cellular location and diurnal rhythm of expression of *Period 1* in the mouse retina. Soc Neurosci Abstr. 2002; 28:177.10.

LeSauter J, Yan L, Vishnubhotla B, Quintero JE, Kuhlman SJ, McMahon DG, Silver R. A short half-life GFP mouse model for analysis of suprachiasmatic nucleus organization. Brain Res. 2003; 964:279–287. [PubMed: 12576188]

Miyamoto Y, Sancar A. Vitamin B_2-based blue-light photoreceptors in the retinohypothalamic tract as the photoactive pigments for setting the circadian clock in mammals. Proc Natl Acad Sci USA. 1998; 95:6097–6102. [PubMed: 9600923]

Namihira M, Honma S, Abe H, Masubuchi S, Ikeda M, Honmaca K. Circadian pattern, light responsiveness, and localization of *rPer1* and *rPer2* gene expression in the rat retina. NeuroReport. 2001; 12:471–475. [PubMed: 11234748]

Niki T, Hamada T, Ohtomi M, Sakamoto K, Suzuki S, Kako K, Hosoya Y, Horikawa K, Ishida N. The localization of the site of arylaklylamine *N*-acetyltransferase circadian expression in the photoreceptor cells of mammalian retina. Biochem Biophys Res Commun. 1998; 248:115–120. [PubMed: 9675096]

Pierce ME, Sheshberadaran H, Zhang Z, Fox LE, Applebury ML, Takahashi JS. Circadian regulation of iodopsin gene expression in embryonic photoreceptors in retinal cell culture. Neuron. 1993; 10:579–584. [PubMed: 8476610]

Provencio I, Rollag MD, Castrucci AM. Photoreceptive net in the mammalian retina. Nature. 2002; 415:493. [PubMed: 11823848]

Shearman LP, Zylka MJ, Weaver DR, Kolakowski LF, Reppert SM. Two *period* homologs: circadian expression and photic regulation in the suprachiasmatic nuclei. Neuron. 1997; 19:1261–1269. [PubMed: 9427249]

Shindler KS, Roth KA. Double immunofluorescent staining using two unconjugated primary antisera raised in the same species. J Histochem Cytochem. 1996; 44:1331–1335. [PubMed: 8918908]

Terman JS, Reme CE, Terman M. Rod outer segment disk shedding in rats with lesions of the suprachiasmatic nucleus. Brain Res. 1993; 605:256–264. [PubMed: 8481775]

Tosini G, Fukuhara C. The mammalian retina as a clock. Cell Tissue Res. 2002; 309:119–126. [PubMed: 12111542]

Tosini G, Menaker M. Circadian rhythms in cultured mammalian retina. Science. 1996; 272:419–421. [PubMed: 8602533]

Van der Horst GTJ, Muijtjens M, Kobayashi K, Takano R, Kanno S, Takao M, de Wit J, Verkert A, Eker APM, van Leenen D, Juijs R, Bootsma D, Hoeijmakers JHJ, Yasui A. Mammalian *Cry1* and *Cry2* are essential for maintenance of circadian rhythms. Nature. 1999; 398:627–630. [PubMed: 10217146]

Witkovsky P, Schuette M. The organization of dopaminergic neurons in vertebrate retinas. Vis Neurosci. 1991; 7:113–124. [PubMed: 1931794]

Yan L, Silver R. Differential induction and localization of *mPer1* and *mPer2* during advancing and delaying phase shifts. Eur J Neurosci. 2002; 16:1531–1540. [PubMed: 12405967]

Yan L, Takekida S, Shigeyoshi Y, Okamura H. *Per1* and *Per2* gene expression in the rat suprachiasmatic nucleus: circadian profile and the compartment-specific response to light. Neuroscience. 1999; 94:141–150. [PubMed: 10613504]

Zhu H, La Rue S, Whiteley A, Steeves TD, Takahashi J, Green CB. The *Xenopus* clock gene is constitutively expressed in retinal photoreceptors. Brain Res Mol Brain Res. 2000; 75:303–308. [PubMed: 10686352]

Zhuang M, Wang Y, Steenhard BM, Besharse JC. Differential regulation of two *Period* genes in the *Xenopus* eye. Mol Brain Res. 2000; 82:52–64. [PubMed: 11042357]

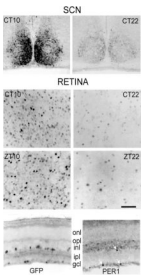

Figure 1.

GFP-IR in the retina and SCN. Shown are coronal sections of the SCN (top row) and flat-mount views of the retina focused on the border of inner nuclear and inner plexiform layers (second row) from the same mice killed at CT 10 or CT 22, as indicated. The staining intensity varies markedly from cell to cell, but the fraction of cells with strong GFP-IR is much greater at CT 10 than at CT 22. Shown in the third row are identical flat-mount view of the retinas from mice killed at ZT 10 or ZT 22. In the fourth row, left, is a vertical section of retina showing GFP-IR in neurons at the border of inner nuclear and inner plexiform layers and in the ganglion cell layer. onl, Outer nuclear (photoreceptor) layer; opl, outer plexiform layer; inl, inner nuclear layer; ipl, inner plexiform layer; gcl, ganglion cell layer. In the fourth row, right, is a vertical section of retina showing PER1-IR. Three arrows mark PER-IR neurons at the INL/IPL border and in the GCL. PER1-IR profiles are smaller than GFP-IR profiles because of the diffusion of GFP in the neuron. Scale bar: retina, 50 μm; SCN, 65 μm.

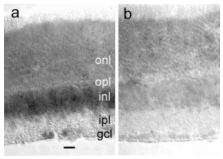

Figure 2.
mPer1 message in the retina. Shown are antisense mRNA (*a*) and sense control (*b*) in vertical retinal sections. Retinal layer abbreviations are the same as for Figure 1. Note increased antisense staining in inner nuclear and ganglion cell layers and the absence of staining in the outer nuclear (photoreceptor) layer. Scale bar, 20μm.

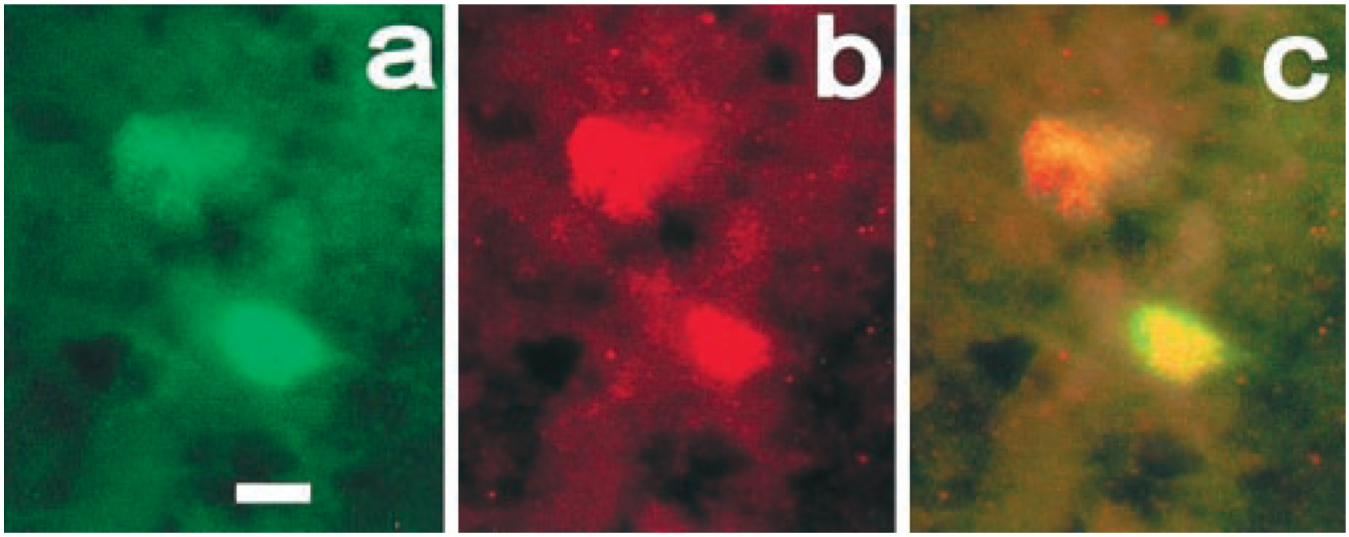

Figure 3.
Colocalization of GFP-IR and PER1-IR in retinal neurons. Shown are confocal images of GFP-IR (*a*, green) and PER1-IR (*b*, red) in amacrine cell perikarya. The two images are superimposed in *c*, showing colocalization (yellow to orange). Scale bar, 10μm.

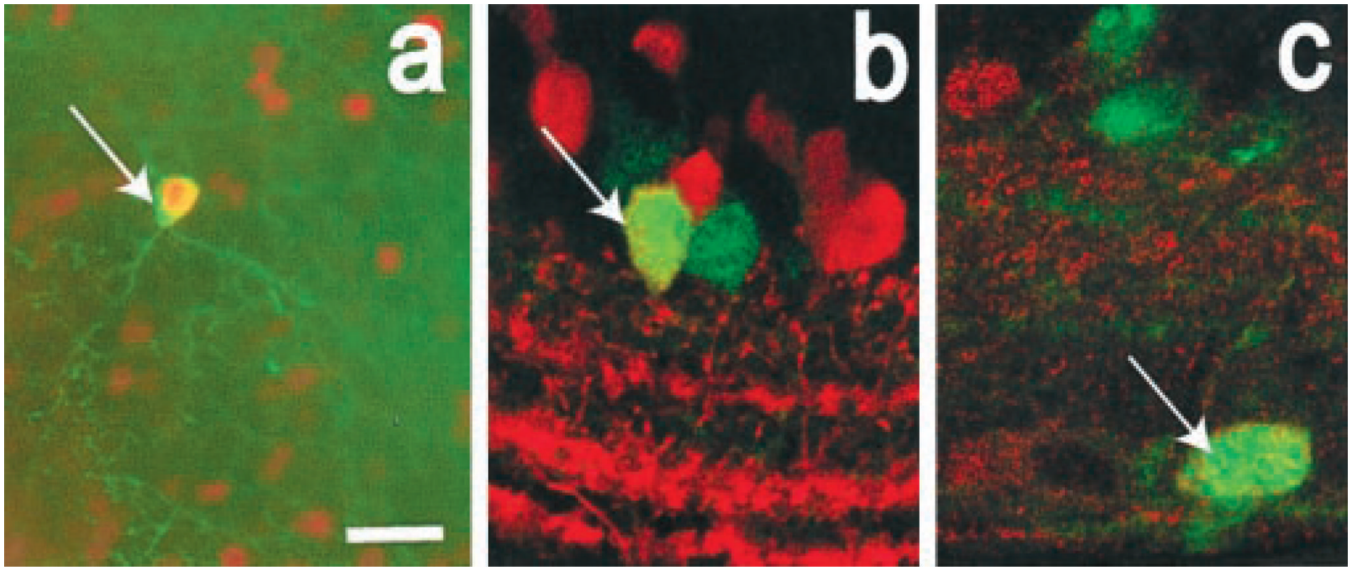

Figure 4.

Colocalization of GFP with marker proteins in retinal amacrine cells. *a*, Flat-mount view showing tyrosine hydroxylase (TH)-IR (green) and GFP-IR (orange). The arrow indicates a TH^+ perikaryon in which GFP-IR is colocalized. *b*, Vertical section of the retina showing GFP-IR (green), calretinin-IR (red), and colocalization of these two in one neuron (arrow). Note $calretinin^+$ processes in bands within the inner plexiform layer. *c*, Vertical retinal section showing GFP-IR (green), calbindin-IR (red), and their colocalization in one neuron (arrow). Scale bar (in *a*) *a*, 25 μm; *b*, *c*, 10 μm.

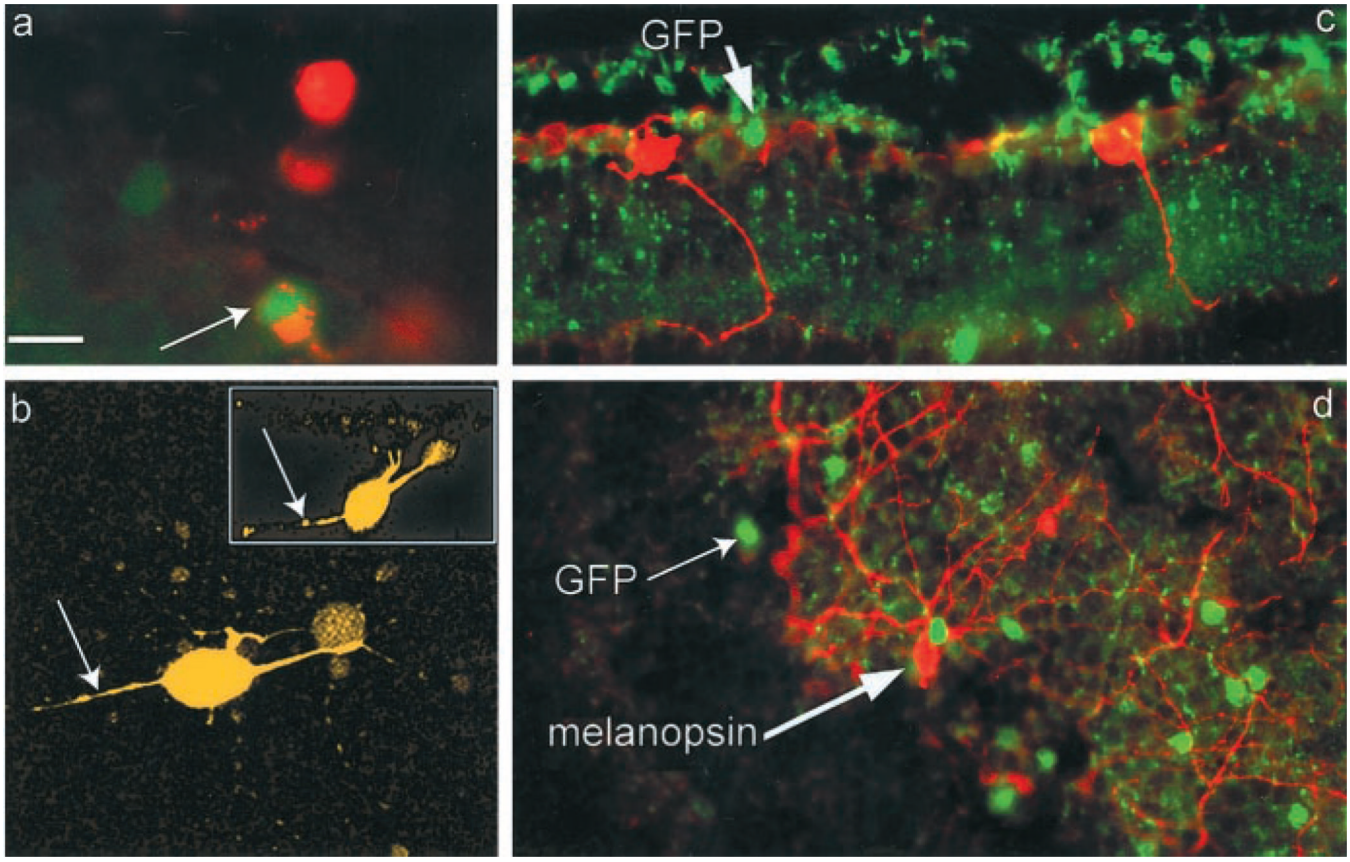

Figure 5.

Some ganglion cells express *Per-1*-driven GFP. *a*, Fluorescence image of retinal ganglion cells labeled by retrograde transport of the dye DiI from the superior colliculus (red) and GFP^+ neurons in the ganglion cell layer (green). Per1-driven GFP filled the entire somata of neurons, whereas DiI tended to label the cell bodies of individual neurons partially. A neuron double-labeled with GFP and DiI (yellow) is indicated by an arrow. *b*, Confocal image of a GFP^+ neuron in the ganglion cell layer of a retinal whole mount filled with Lucifer yellow. The axon of the cell exits from the left side of the ganglion cell body (arrow). Inset, A vertical view of this same cell generated by three-dimensional rotation of the *z*-stack of confocal images taken in the flat mount. The axon is visible extending downward to the nerve fiber layer (arrow), whereas the primary dendrites extend upward toward the inner plexiform layer. *c*, Vertical retinal section with merged images of melanopsin-IR (red) and GFP-IR (green). The melanopsin neurons lack GFP-IR *d*, Tangential section through the retina showing a $melanopsin^+$ neuron for which the cell body is at the border of inner nuclear and inner plexiform layers. This neuron lacks GFP-IR, although many neighboring perikarya show GFP-IR (green profiles). Scale bar: (in *a*) *a*, *b*, 10 μm; *c*, 20 μm; *d*, 30 μm.

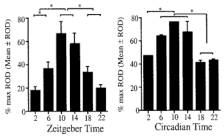

Figure 6.

Relative optical density (ROD) of GFP-IR in retina. GFP-IR was measured as a ROD signal. Background signals were subtracted, and the values for each tissue were scaled (see Materials and Methods). Vertical bars show ROD values (mean ± 1 SE) for retinal amacrine neurons as a function of the Zeitgeber (left) or circadian time (right) at which the tissues were harvested. In both groups ROD peaked near ZT 10. Single asterisks indicate 95% confidence level for a significant difference between the indicated vertical bars.

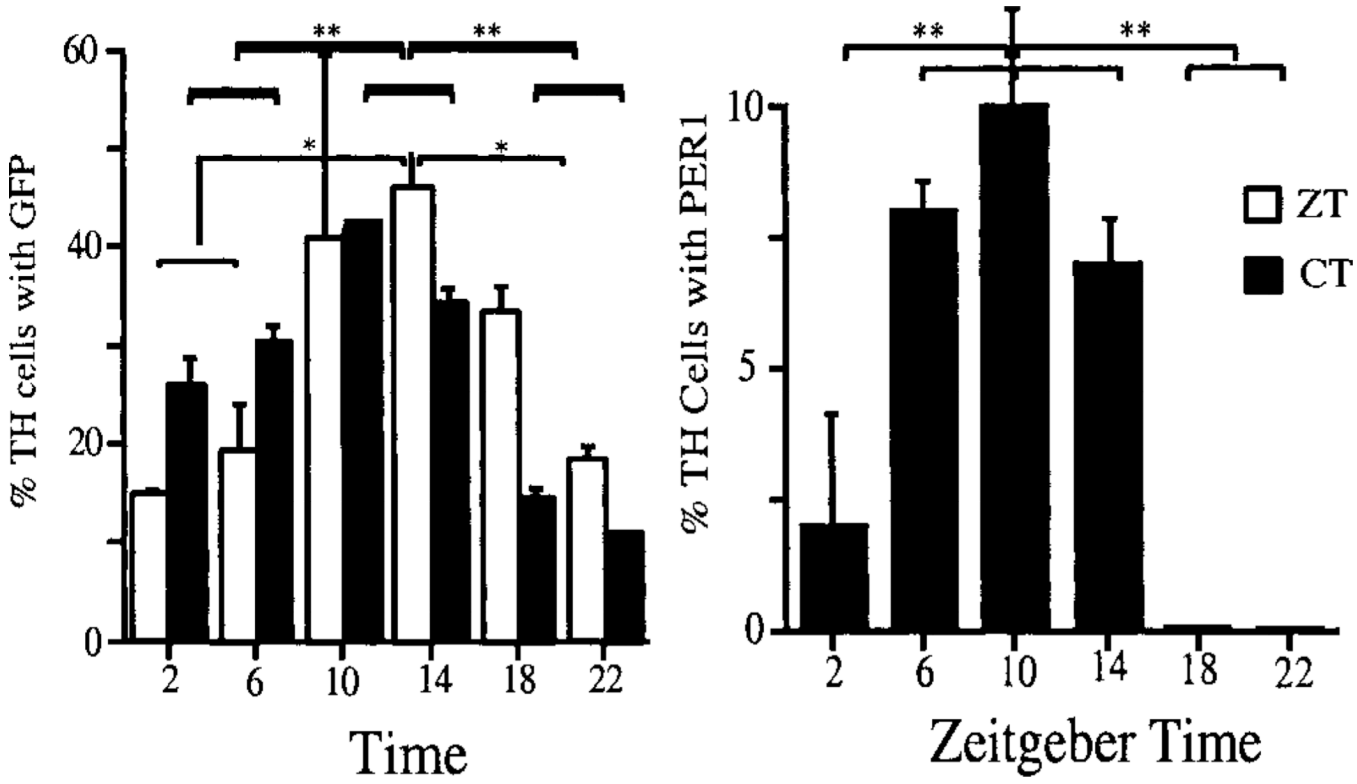

Figure 7.

Diurnal and circadian rhythms of GFP-IR and PER1-IR in TH amacrine cells. Retinas were harvested at ZT 2, 6, 10, 14, 18, and 22. For GFP only, an identical series was obtained at CT 2, 6, 10, 14, 18, and 22. Two mice were used per time point, and the values were averaged. For the ZT series one retina/mouse was reacted for GFP-IR and the other for PER1-IR. Then 100 TH cells/retina were examined for GFP (left) or PER1-IR (right). No PER1-IR was detected at ZT 18 or ZT 22. Single asterisks indicate 95% confidence level; double asterisks indicate 99% confidence level for a significant difference between the indicated pairs.